



Evidence for a Magnetic Seebeck Effect

Sylvain D. Brechet,^{1,*} Francesco A. Vetro,¹ Elisa Papa,¹ Stewart E. Barnes,² and Jean-Philippe Ansermet¹

¹*Institute of Condensed Matter Physics, Station 3, Ecole Polytechnique Fédérale de Lausanne—EPFL, CH-1015 Lausanne, Switzerland*

²*James L. Knight Physics Building, 1320 Campo Sano Avenue, University of Miami, Coral Gables, Florida 33124, USA*

(Received 5 June 2013; published 22 August 2013)

The irreversible thermodynamics of a continuous medium with magnetic dipoles predicts that a temperature gradient in the presence of magnetization waves induces a magnetic induction field, which is the magnetic analog of the Seebeck effect. This thermal gradient modulates the precession and relaxation. The magnetic Seebeck effect implies that magnetization waves propagating in the direction of the temperature gradient and the external magnetic induction field are less attenuated, while magnetization waves propagating in the opposite direction are more attenuated.

DOI: [10.1103/PhysRevLett.111.087205](https://doi.org/10.1103/PhysRevLett.111.087205)

PACS numbers: 75.76.+j, 76.50.+g

The discovery of the spin Seebeck effects in ferromagnetic metals [1], in semiconductors [2], and in insulators [3] has generated much research for spin transport in ferromagnetic samples of macroscopic dimensions subjected to temperature gradients. The interplay of spin, charge, and heat transport defines the rich field known as spin caloritronics [4]. Prompted by these recent developments, we established a formalism describing the irreversible thermodynamics of a continuous medium with magnetization [5].

In this Letter, we test a particular experimental prediction of this formalism on a yttrium iron garnet (YIG) slab. We argue that the thermodynamics of irreversible processes implies the existence of a magnetic counterpart to the well-known Seebeck effect. We show how a thermally induced magnetic field modifies the Landau-Lifshitz equation and provide experimental evidence for the magnetic Seebeck effect by the propagation of magnetization waves in thin crystals of YIG. The effect of a temperature gradient on the dynamics of the magnetization on a YIG slab with and without Pt stripes was investigated recently by Obry *et al.* [6], Cunha *et al.* [7], Silva *et al.* [8], Padrón-Hernández *et al.* [9,10], Jungfleisch *et al.* [11], and Lu *et al.* [12].

In general, irreversible thermodynamics predicts couplings between current and force densities. In Eq. (86) of Ref. [5], we identified the magnetization force term $\mathbf{m}\nabla\mathbf{B}$. For an insulator like YIG, there is no charge current. As explained in detail in Ref. [5], the transport equation (94) of Ref. [5] implies that the magnetization force density $\mathbf{M}\nabla\mathbf{B}_{\text{ind}}$ induced by a thermal force density $-nk_B\nabla T$ is proportional and opposite to this force density, i.e.,

$$\mathbf{M}\nabla\mathbf{B}_{\text{ind}} = \lambda nk_B\nabla T, \quad (1)$$

which corresponds to Eq. (155) of Ref. [5], where $\lambda > 0$ is a phenomenological dimensionless parameter, k_B is Boltzmann's constant, and $n = 1.1 \times 10^{28} \text{ m}^{-3}$ is the Bohr magneton number density of YIG. The

thermodynamic formalism does not allow for a direct estimation of λ . The numerical value of this parameter needs to be evaluated directly from the experimental data, as shown below.

In the bulk of the sample, as shown in Ref. [5], the magnetization force density has the structure of a Lorentz force density [13] expressed in terms of the magnetic bound current density $\mathbf{j}_M = \nabla \times \mathbf{M}$ [14]

$$\mathbf{M}\nabla\mathbf{B}_{\text{ind}} = \mathbf{j}_M \times \mathbf{B}_{\text{ind}}. \quad (2)$$

Thus, using vectorial identities, the phenomenological relations (1) and (2) imply that in the bulk of the system, the magnetic induction field \mathbf{B}_{ind} , induced by a uniform temperature gradient ∇T in the presence of a magnetic bound current density $\nabla \times \mathbf{M}$, is given by, i.e.,

$$\mathbf{B}_{\text{ind}} = \boldsymbol{\varepsilon}_M \times \nabla T, \quad (3)$$

where the phenomenological vector $\boldsymbol{\varepsilon}_M$ is given by

$$\boldsymbol{\varepsilon}_M = -\lambda nk_B(\nabla \times \mathbf{M})^{-1}. \quad (4)$$

By analogy with the Seebeck effect, we shall refer to this phenomenon as the magnetic Seebeck effect.

The time evolution of the magnetization \mathbf{M} is given by the Landau-Lifschitz-Gilbert equation, i.e.,

$$\dot{\mathbf{M}} = \gamma \mathbf{M} \times \mathbf{B}_{\text{eff}} - \frac{\alpha}{M_S} \mathbf{M} \times \dot{\mathbf{M}}, \quad (5)$$

where γ is the gyromagnetic ratio, $\alpha \approx 10^{-4}$ is the Gilbert damping parameter of YIG [15], and $M_S = 1.4 \times 10^5 \text{ A m}^{-1}$ is the magnitude of the effective saturation magnetization of YIG at room temperature [16]. The effective magnetic induction field \mathbf{B}_{eff} includes the external field \mathbf{B}_{ext} , the demagnetizing field \mathbf{B}_{dem} , the anisotropy field \mathbf{B}_{ani} , which behaves as an effective saturation magnetization in the linear response [17], and finally a thermally induced field \mathbf{B}_{ind} given by the relation (3). The exchange field \mathbf{B}_{int} [18] is negligible in the following, as we consider magnetostatic modes [19]. The demagnetizing

field \mathbf{B}_{dem} breaks the spatial symmetry and generates an elliptic precession cone. After performing the linear response of the magnetization in the presence of a thermally induced field \mathbf{B}_{ind} , we shall describe how the demagnetizing field \mathbf{B}_{dem} affects the magnetic susceptibility.

We found evidence for the magnetic Seebeck effect by exciting locally, at angular frequency $\omega \approx 2.74 \times 10^{10} \text{ s}^{-1}$, the ferromagnetic resonance of a YIG slab of length $L_z = 10^{-2} \text{ m}$, width $L_y = 2 \times 10^{-3} \text{ m}$, and thickness $L_x = 2.5 \times 10^{-5} \text{ m}$, subjected to a temperature gradient as small as $|\nabla T| \approx 2 \times 10^3 \text{ K m}^{-1}$ generated by Peltier elements. The excitation field is applied on the slab using a local antenna, as detailed in Ref. [20]. For signal transmission experiments, two antennas are used, set approximately 8 mm apart, as shown in Fig. 1. Note that a similar setup for a gradient orthogonal to the YIG slab was investigated recently [7]. For reasons explained below, these two setups can be expected to probe different mechanisms.

The external magnetic induction field \mathbf{B}_{ext} applied on the YIG film consists of a uniform and constant field \mathbf{B}_0 and a small excitation field $\mathbf{b} = b_x \hat{\mathbf{x}} + b_y \hat{\mathbf{y}}$ locally oscillating in a plane orthogonal to $\mathbf{B}_0 = B_0 \hat{\mathbf{z}}$. In the limit of a small excitation field, i.e., in the linear limit, the magnetization field \mathbf{M} consists of a uniform and constant field $\mathbf{M}_S = M_S \hat{\mathbf{z}}$ and a response field $\mathbf{m} = m_x \hat{\mathbf{x}} + m_y \hat{\mathbf{y}}$ locally oscillating in a plane orthogonal to \mathbf{M}_S such that $\mathbf{m} \ll \mathbf{M}_S$. The linear response of the magnetization to the excitation field, according to the time evolution equation (5), is given by

$$\dot{\mathbf{m}} = \gamma(\mathbf{m} \times \mathbf{B}_0 + \mathbf{M}_S \times \mathbf{B}_1) - \frac{\alpha}{M_S} \mathbf{M}_S \times \dot{\mathbf{m}}, \quad (6)$$

where the first-order magnetic induction field \mathbf{B}_1 yields

$$\mathbf{B}_1 = \mathbf{b} - \mu_0(\mathbf{k}_T \cdot \nabla^{-1})\mathbf{m}, \quad (7)$$

and μ_0 is the magnetic permeability of vacuum and the thermal wave vector

$$\mathbf{k}_T = \frac{\lambda n k_B}{\mu_0 M_S^2} \nabla T. \quad (8)$$

To obtain the expressions (7) and (8), we used the linear vectorial identity

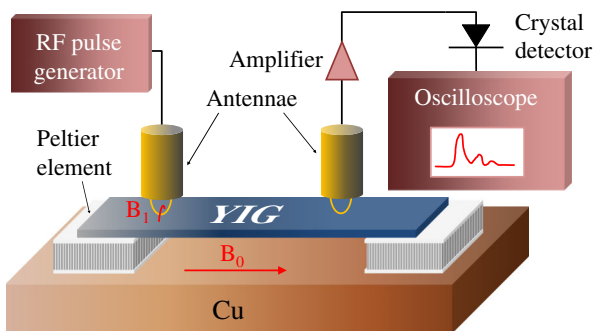


FIG. 1 (color online). Time-resolved transmission measurement of magnetization waves.

$$\begin{aligned} (\nabla \times \mathbf{M})^{-1} \times \nabla T &= \frac{1}{M_S^2} (\nabla^{-1} \times \mathbf{m}) \times \nabla T \\ &= \frac{1}{M_S^2} (\nabla T \cdot \nabla^{-1}) \mathbf{m} - \frac{1}{M_S^2} (\nabla T) \nabla^{-1} \mathbf{m}, \end{aligned}$$

where $\nabla^{-1} \cdot \nabla = 1$ and the last term on the right-hand side vanishes since it averages out on a precession cycle.

The vectorial time evolution equation (6) is written explicitly in Cartesian coordinates as

$$\begin{aligned} \dot{m}_x &= (\omega_0 + \omega_M \mathbf{k}_T \cdot \nabla^{-1}) m_y + \alpha \dot{m}_y - \omega_M \mu_0^{-1} b_y, \\ \dot{m}_y &= -(\omega_0 + \omega_M \mathbf{k}_T \cdot \nabla^{-1}) m_x - \alpha \dot{m}_x + \omega_M \mu_0^{-1} b_x, \end{aligned} \quad (9)$$

where the angular frequencies ω_0 and ω_M are defined, respectively, as

$$\omega_0 = \gamma B_0, \quad \omega_M = \gamma \mu_0 M_S. \quad (10)$$

In a stationary regime, the magnetic excitation field \mathbf{b} and the magnetization response \mathbf{m} are oscillating at an angular frequency ω , which is expressed in Fourier series as

$$\begin{aligned} b_x &= \sum_{\mathbf{k}} b_{\mathbf{k}} e^{i[\mathbf{k} \cdot \mathbf{x} - \omega t + (\pi/2)]}, & b_y &= \sum_{\mathbf{k}} b_{\mathbf{k}} e^{i(\mathbf{k} \cdot \mathbf{x} - \omega t)}, \\ m_x &= \sum_{\mathbf{k}} m_{\mathbf{k}} e^{i[\mathbf{k} \cdot \mathbf{x} - \omega t + (\pi/2)]}, & m_y &= \sum_{\mathbf{k}} m_{\mathbf{k}} e^{i(\mathbf{k} \cdot \mathbf{x} - \omega t)}, \end{aligned} \quad (11)$$

where the eigenstates $b_{\mathbf{k}}$ and $m_{\mathbf{k}}$ are complex valued and dephased.

The Cartesian components of the eigenmodes $k_{x,y,z}$ satisfy the boundary conditions of null \mathbf{m} at the surface of the sample

$$k_{x,y,z} = \frac{n_{x,y,z} \pi}{L_{x,y,z}}, \quad (12)$$

where $n_{x,y,z} \in \mathbb{N}$ [20].

The eigenstates of the excitation field $b_{\mathbf{k}}$ and the response field $m_{\mathbf{k}}$ are related through the magnetic susceptibility $\chi_{\mathbf{k}}$, i.e.,

$$m_{\mathbf{k}} = \mu_0^{-1} \chi_{\mathbf{k}} b_{\mathbf{k}}. \quad (13)$$

The time evolution equations (9), the definition (10), and the Fourier series (11) in the stationary regime imply that the magnetic susceptibility $\chi_{\mathbf{k}}$ is given by

$$\chi_{\mathbf{k}} = -\frac{1}{\Omega - \Omega_0 + i(\alpha \Omega + \mathbf{k}_T \cdot \mathbf{k}^{-1})}, \quad (14)$$

where the dimensionless parameters Ω and Ω_0 are, respectively, defined as

$$\Omega = \frac{\omega}{\omega_M}, \quad \Omega_0 = \frac{\omega_0}{\omega_M}. \quad (15)$$

The demagnetizing field $\mathbf{B}_{\text{dem}} = -\mu_0 m_x \hat{\mathbf{x}}$ causes the damping and the magnetic susceptibility $\chi_{\mathbf{k}_x}$ along the x axis to differ respectively from the damping and

the magnetic susceptibility χ_{ky} along the y axis. The resonance frequency $\sqrt{\omega_0(\omega_0 + \omega_M)}$ is given by Kittel's formula [21] to first order in α and \mathbf{k}_T . Thus, the magnetic susceptibilities $\chi_{kx,y}$ yield

$$\chi_{kx,y} = -\frac{1}{\Omega - \sqrt{\Omega_0(\Omega_0 + 1)} + ir_{x,y}(\alpha\Omega + \mathbf{k}_T \cdot \mathbf{k}^{-1})}, \quad (16)$$

where $r_{x,y} > 0$ are phenomenological damping scale factors accounting for symmetry breaking.

As shown by Cunha *et al.* in Fig. 1(a) of Ref. [7], the propagating modes of the magnetization waves in the bulk of YIG are magnetostatic backward volume modes propagating in the direction $-\mathbf{k}^{-1}$. The expressions (8) and (16) for the magnetic susceptibilities and the thermal wave vector \mathbf{k}_T imply that the magnetization waves propagating from the cold to the hot side, i.e., $\mathbf{k}_T \cdot \mathbf{k}^{-1} < 0$, are less attenuated by the temperature gradient and the magnetization waves propagating from the hot to the cold sides, i.e., $\mathbf{k}_T \cdot \mathbf{k}^{-1} > 0$, are further attenuated.

Thus, the opening angle of the precession cone of the magnetization \mathbf{m} for a magnetization wave propagating in the direction of the temperature gradient decreases less

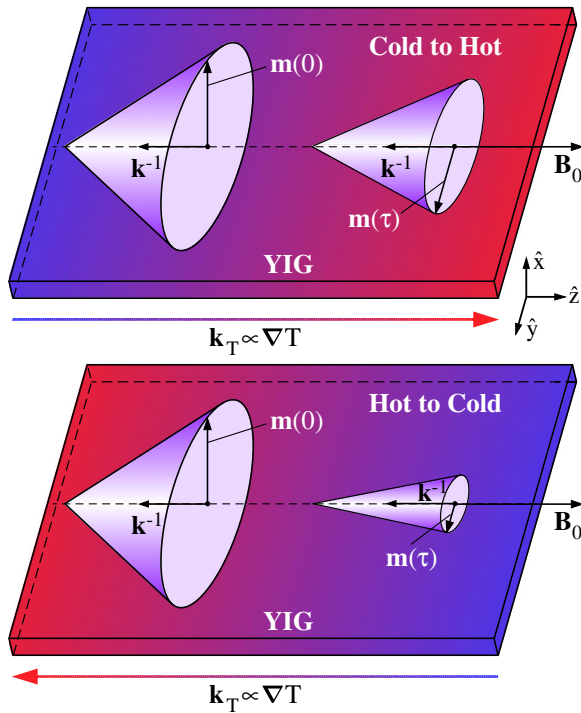


FIG. 2 (color online). Propagation of magnetization waves from the cold to the hot side (top) and vice versa (bottom). The cones describe the precession of the magnetization at excitation $\mathbf{m}(0)$ and at detection $\mathbf{m}(\tau)$. The amount of damping depends on the relative orientation \mathbf{k}_T of the temperature gradient with respect to the magnetization wave propagation direction $-\mathbf{k}^{-1}$.

than the opening angle for a magnetization wave propagating in the opposite direction, as shown in Fig. 2.

This is confirmed experimentally by detecting inductively at one end of the sample the signal that results from an excitation pulse of 15 ns duration at the other end. The signals obtained by sweeping the magnetic induction field \mathbf{B}_0 for the propagation of magnetization waves from the cold end to the hot end or from the hot end to the cold end are given in Fig. 3. Clearly, the waves propagating from the cold to the hot side appear to decay less rapidly than the waves propagating from the hot to the cold side.

The time evolution of the signals for the waves propagating in the direction of the gradient or opposite to it is obtained by averaging the signals over the range of the magnetic induction field \mathbf{B}_0 displayed in Fig. 4. The signal is a convolution of k_z modes that have different group velocities and decay exponentially due to the damping. The peaks were identified in Ref. [22] as the result of the propagation of odd modes. Since the peaks of the transmitted signals are detected at the same time, the temperature gradient does not affect significantly the k_z mode group velocities. Moreover, from the logarithmic scale for the signal in Fig. 4, a larger difference in attenuation between the signals for small k_z modes is inferred. This is in line with the theoretical prediction, made by Eq. (16), for the magnetic Seebeck effect to be proportional to k_z^{-1} . Moreover, since the relative difference between the signals is due to the temperature gradient, we can estimate the relative difference between the damping terms $\alpha\Omega$ and

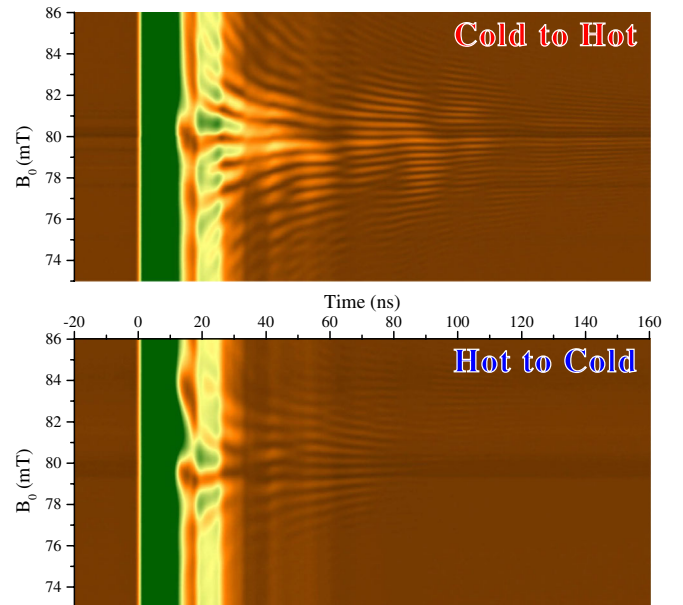


FIG. 3 (color online). Transmitted signals from the cold to the hot side and from the hot to the cold side as a function of the magnetic field \mathbf{B}_0 and of the detection time after a 15 ns pulsed excitation at 4.36 GHz. The lighter areas correspond to a larger signal.

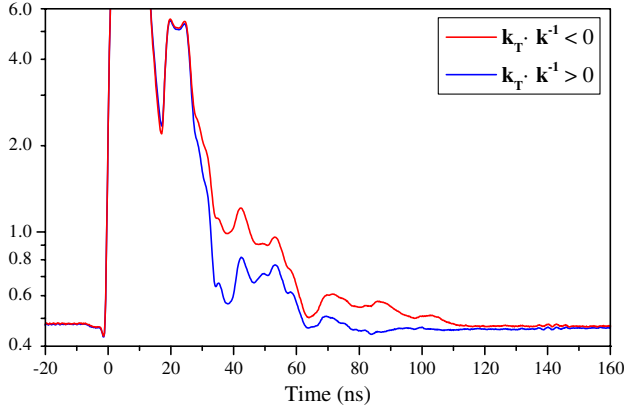


FIG. 4 (color online). Transmitted signal as a function of time after a 15 ns pulsed excitation at 4.36 GHz.

$\mathbf{k}_T \cdot \mathbf{k}^{-1}$ appearing in the expression (16) for the magnetic susceptibilities. Comparing the signals at $t = 40$ ns, we find that the dimensionless parameter $\lambda \simeq 6 \times 10^{-7}$, which corresponds to a thermal damping ratio $|\mathbf{k}_T \cdot \mathbf{k}^{-1}|/\alpha\Omega \simeq 0.3$ less than an order of magnitude below the self-oscillation threshold.

The difference in attenuation between the signals is also shown on the ferromagnetic resonance (FMR) spectrum detected 70 ns after the pulse and displayed in Fig. 5. The spectral linewidth ~ 0.2 mT corresponds to inhomogeneous broadening, since it is much larger than the homogeneous linewidth $\sim \alpha B_{\text{eff}}$ [23].

As is rightly pointed out in Ref. [6], the temperature dependence of the saturation magnetization affects the amplitude of the magnetization waves. However, since our experimental setup is sufficiently close to the self-oscillation threshold for a temperature gradient that is small enough, we expect the dynamic contribution $\mathbf{k}_T \cdot \mathbf{k}^{-1}$ to be larger than the static contribution due to the temperature dependence of the saturation magnetization. Moreover, in contrast to the claim made in Ref. [6], Fig. 4 shows that magnetization waves can propagate with and

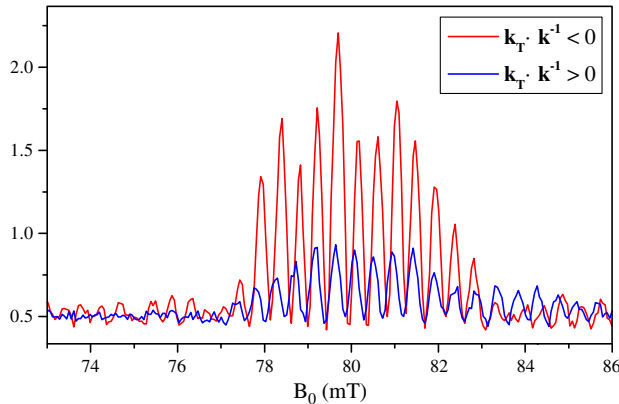


FIG. 5 (color online). FMR signal of a 15 ns pulsed excitation at 4.36 GHz detected after 70 ns, after baseline correction.

against the temperature gradient and that the effect of the temperature is proportional to k_z^{-1} .

For a temperature gradient orthogonal to the YIG plane, Cunha *et al.* [7] showed that the temperature gradient affects the propagation of magnetization waves only when Pt is deposited on the YIG slab. The effect is accounted for by a model of spin injection and spin pumping, detailed by Ando *et al.* [24], at the interface between Pt and YIG. The quantitative analysis of the data is presented in Ref. [8]. In Ref. [7], it is stated clearly that the effect does not occur in the absence of Pt on the surface. When Pt is removed in such a setup where $\mathbf{k}_T \cdot \mathbf{k}^{-1} = 0$, the mechanism invoked by Cunha *et al.* is not operative and our mechanism is not effective either.

In summary, we point out that thermodynamics of irreversible processes implies a coupling between heat current and magnetization precession in a temperature gradient. This effect can be expressed by an induced magnetic field \mathbf{B}_{ind} proportional to the applied temperature gradient. Thus, we suggest to refer to it as a magnetic Seebeck effect, since it is the magnetic analog of the regular Seebeck effect. It is distinct from the magneto-Seebeck effect, which refers to a change in the Seebeck coefficient due to the magnetic response of nanostructures [25]. We analyze how the Landau-Lifshitz equation is modified and find a contribution to the dissipation that is linear in ∇T . Hence, this effect can increase or decrease the damping, depending on the orientation of the wave vector of the excited magnetostatic mode with respect to the temperature gradient. If the temperature gradient could be made strong enough, i.e., $\mathbf{k}_T \cdot \mathbf{k}^{-1} > \alpha\Omega$, then the damping would be negative and the magnetization would undergo self-oscillation. This would be analogous to the magnetization self-oscillation described in Chap. 7 of Ref. [26] and the heat equivalent of Berger's spin amplification by simulated emission of radiation (SWASER) predicted for charge-driven spin polarized currents [27].

We thank François A. Reuse, Klaus Maschke, and Joseph Heremans for insightful comments and acknowledge the following funding agencies: Polish-Swiss Research Program NANOSPIN PSRP-045/2010 and Deutsche Forschungsgemeinschaft SS1538 SPINCAT, Grant No. AN762/1.

*sylvain.brechet@epfl.ch

- [1] K. Uchida, S. Takahashi, K. Harii, J. Ieda, W. Koshibae, K. Ando, S. Maekawa, and E. Saitoh, *Nature (London)* **455**, 778 (2008).
- [2] C. M. Jaworski, J. Yang, S. Mack, D. D. Awschalom, J. P. Heremans, and R. C. Myers, *Nat. Mater.* **9**, 898 (2010).
- [3] K. Uchida, J. Xiao, H. Adachi, J. Ohe, S. Takahashi, J. Ieda, T. Ota, Y. Kajiwara, H. Umezawa, H. Kawai, G. E. W. Bauer, S. Maekawa, and E. Saitoh, *Nat. Mater.* **9**, 894 (2010).

- [4] G. E. W. Bauer, E. Saitoh, and B. J. van Wees, *Nat. Mater.* **11**, 391 (2012).
- [5] S. D. Brechet and J.-P. Ansermet, *Eur. Phys. J. B* **86**, 318 (2013).
- [6] B. Obry, V. I. Vasyuchka, A. V. Chumak, A. A. Serga, and B. Hillebrands, *Appl. Phys. Lett.* **101**, 192406 (2012).
- [7] R. O. Cunha, E. Padrón-Hernández, A. Azevedo, and S. M. Rezende, *Phys. Rev. B* **87**, 184401 (2013).
- [8] G. L. da Silva, L. H. Vilela-Leano, S. M. Rezende, and A. Azevedo, *Appl. Phys. Lett.* **102**, 012401 (2013).
- [9] E. Padrón-Hernández, A. Azevedo, and S. M. Rezende, *J. Appl. Phys.* **111**, 07D504 (2012).
- [10] E. Padrón-Hernández, A. Azevedo, and S. M. Rezende, *Phys. Rev. Lett.* **107**, 197203 (2011).
- [11] M. B. Jungfleisch, T. An, K. Ando, Y. Kajiwara, K. Uchida, V. I. Vasyuchka, A. V. Chumak, A. A. Serga, E. Saitoh, and B. Hillebrands, *Appl. Phys. Lett.* **102**, 062417 (2013).
- [12] L. Lu, Y. Sun, M. Jantz, and M. Wu, *Phys. Rev. Lett.* **108**, 257202 (2012).
- [13] F. A. Reuse, *Electrodynamique* (PPUR, Lausanne, 2012).
- [14] D. J. Griffiths, *Introduction to Electrodynamics* (Prentice-Hall, Upper Saddle River, 1999), 3rd ed.
- [15] H. Kurebayashi, O. Dzyapko, V. E. Demidov, D. Fang, A. J. Ferguson, and S. O. Demokritov, *Nat. Mater.* **10**, 660 (2011).
- [16] F. Boukchiche, T. Zhou, M. L. Berre, D. Vincent, B. Payet-Gervy, and F. Calmon, *Proceedings of PIERS 2010 in Cambridge* (MIT Press, Cambridge, MA, 2010), Vol. 1, p. 700.
- [17] J. A. Duncan, B. E. Storey, A. O. Tooke, and A. P. Cracknell, *J. Phys. C* **13**, 2079 (1980).
- [18] C. Kittel, *Rev. Mod. Phys.* **21**, 541 (1949).
- [19] A. A. Serga, A. V. Chumak, and B. Hillebrands, *J. Phys. D* **43**, 264002 (2010).
- [20] E. Papa, S. E. Barnes, and J.-P. Ansermet, *IEEE Trans. Magn.* **49**, 1055 (2013).
- [21] C. Kittel, *Introduction to Solid State Physics* (Wiley, New York, 2004), 8th ed.
- [22] E. Padrón-Hernández, A. Azevedo, and S. M. Rezende, *Appl. Phys. Lett.* **99**, 192511 (2011).
- [23] S. V. Vonsovskii, *Ferromagnetic Resonance* (Pergamon, Oxford, 1966).
- [24] K. Ando, S. Takahashi, K. Harii, K. Sasage, J. Ieda, S. Maekawa, and E. Saitoh, *Phys. Rev. Lett.* **101**, 036601 (2008).
- [25] M. Walter, J. Walowski, V. Zbarsky, M. Munzenberg, M. Schafers, D. Ebke, G. Reiss, A. Thomas, P. Peretzki, M. Seibt, J. S. Moodera, M. Czerner, M. Bachmann, and C. Heiliger, *Nat. Mater.* **10**, 742 (2011).
- [26] S. E. Barnes, *Spin Current*, edited by S. Maekawa, S. O. Valenzuela, E. Saitoh, and T. Kimura (Oxford University Press, New York, 2012).
- [27] L. Berger, *IEEE Trans. Magn.* **34**, 3837 (1998).